A Numerical Study of THz Emission Properties of Arsenic-ion-implanted GaAs Based Photoconductive Antennas

Phumin Kirawanich
Electrical Engineering Department, Mahidol University
Salaya, Nakhon Pathom 73170 Thailand, egphumin@staff2.mahidol.ac.th

1. Introduction

Radiation from far-infrared region of the electromagnetic spectrum is of great importance for time-resolved terahertz (THz) spectroscopy and imaging to provide a non-invasive method for identifying the compositions of non-conducting objects. Applications of sub-millimetre wave technology include medical imaging, bioscience, surveillance and security screening, and pharmaceutical science. The tool generating terahertz wave is usually an antenna based on the photoconductive (PC) switch, which consists of a semiconductor bridging the gap in a transmission line structure deposited on the semiconductor substrate [1]. An ultra short optical pulse focused onto the gap between two voltage-biased electrodes initiates the transient response of the photoconductive switch. The induced photocurrent then radiates into free space proportional to its time derivative. Low temperature grown GaAs (LT-GaAs) is preferred as the substrate of PC antennas due to a short carrier lifetime and reasonably good mobility that can produce ultra-short current pulses of less than picoseconds FWHM [2]. An alternative arsenic-rich material known as arsenic-ion-implanted GaAs (GaAs:As^+) has recently been reported [3]. The GaAs:As^+ exhibits structural, electrical, and ultrafast optoelectronic characteristics similar to those of LT-GaAs due to the presence of the implantation-induced defects. The advantage of GaAs:As^+ over the LT-GaAs is the substrate preparation by ion implantation, which can be controlled more precisely than the epitaxial growth temperature of LT-GaAs. Thus, GaAs:As^+ is expected to work as an efficient substrate for the PC antennas. For that reason, gaining an insight of the device performance through a preliminary numerical design is essential. The limitation of commercially available software is lacking of integrated interactions between the emitter and the semiconductor. In this paper we report on a numerical analysis of an ultrashort pulse emission by taking into account such interactions by incorporating between Maxwell's curl and semiconductor carrier transport equations. We have organized the paper as follows. The details of PC antenna model and computation algorithm are described in Section 2. Section 3 discusses the numerical results. This work concludes in Section 4.

2. PC Antenna Model

Fig. 1 shows the arrangement of PC antenna used in this analysis where the parameters are L = 50 μm, H = 50 μm, G = 5 μm, D = 10 μm, and W = 20 μm. The location of optical excitation is at the center between inside the gap G.

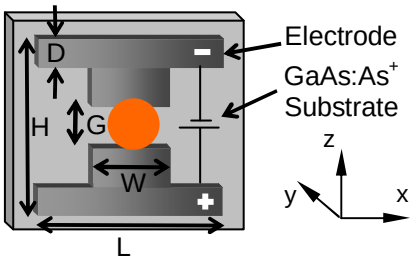

Figure 1: Geometry of PC antenna under the bias voltage in the rectangular coordinate.

The simulation process, as shown by the flowchart in Fig. 2, starts by initializing the steady-state solutions of electric field E_0 and carrier densities (n_0, p_0) by solving through 3-D Poisson equation. The iterative algorithm then proceeds with the time-domain calculations for wave interaction and carrier generation. The iteration starts by solving at each time step variable electric and magnetic fields ($E(t)$, $H(t)$) from Maxwell curl equations, the electron–hole current densities ($J_n(t)$, $J_p(t)$), and the electron–hole concentrations ($n(t)$, $p(t)$) from drift–diffusion current and continuity equations.

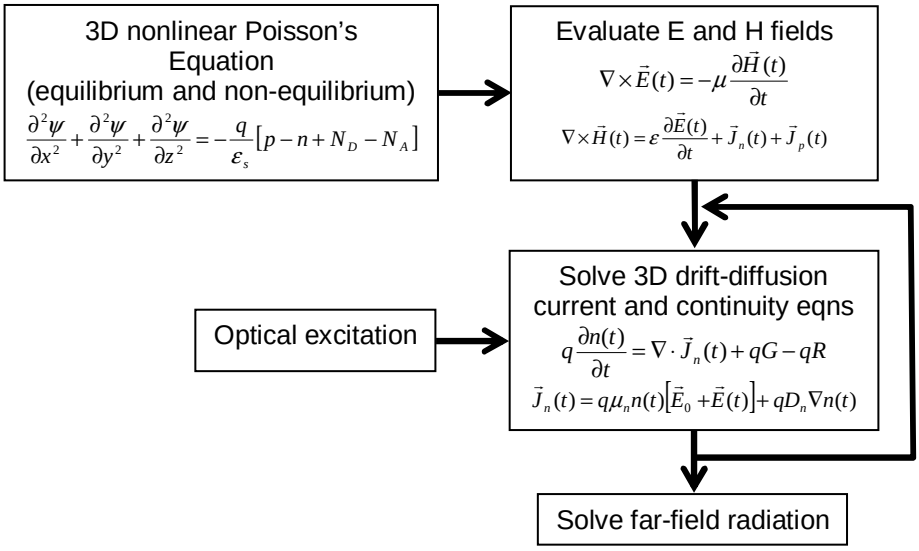

Figure 2: Flowchart describing the sequence of electromagnetic wave and carrier transport calculations.

The process is updated in time in response to applied optical pulse excitation and carried on until the end of simulation. The output power of the emitted far-field THz pulse is affected by the applied bias voltage, pump laser power, antenna pattern, and mobility of the photoconductor. To obtain the far-zone electric fields, we used the near field-to-far field transformation technique using the virtual surface enclosing the entire emitting structure. The THz generation system is simulated through in-house 3D FDTD-based codes. The computational volume is 50 × 20 × 50 μm^3 with a five-layer uniaxial perfectly matched layer. For the Maxwell curl equations, the spatial step size in micrometer seems to be reasonable since the factor of at least ten times smaller than the propagation wavelengths still holds. However, the carrier transport equations are more sensitive to the spatial sampling, requiring only a few nanometer space steps. The satisfying solution is to compromise with the step size Δ of 200 nm without a need of separating computation domains. Thus, an associated computation domain of 250 × 100 × 250 was used in this work. The time step is determined by $\Delta t = S_c\Delta/c$, where c is the wave speed in vacuum and S_c is the Courant stability condition number for which we chose $S_c = 0.5$ in our calculations.

3. Numerical Results

An GaAs:As^+ photoconductive n type material with reasonably high mobility of 300 cm^2/V.s and carrier trapping time as short as 0.1 ps for implantation dosage of 10^{12} ions/cm^2 were used in simulations [4]. Once trapped, carriers are unable to escape the defect via thermal excitation, and that trapped carriers do not alter free carrier states. The spatial and time step sizes chosen are smaller than the Debye length and dielectric relaxation time, respectively. The electrodes of the antenna are perfect electric conductors oppositely voltage biased of ± 30 V. The PC antennas is excited within the area indicated in Fig. 1 by the y-directed optical pulses with a pulse width of 80 fs (FWHM), a photon density of 0.5 W/μm^2, and a wavelength of 780 nm related to the absorption coefficient of ~ 10^4 cm^{-1} [5]. The THz generation system is simulated through an in house code developed on a PC running with a 64-bit quad-core processor.

For the initial simulation, the steady-state electric field is obtained by solving the second-order partial derivatives of the nonlinear Poisson's equation realized in terms of finite difference forms using the central difference scheme and the quasi-linearization approximation. We carried out the calculation for 500 iterations by gradually increasing the applied voltage, causing the charge to redistribute over the entire device volume with Neumann and Dirichlet boundaries. Fig. 3 shows the steady-state results of the electric field E_0 cut through x_c.

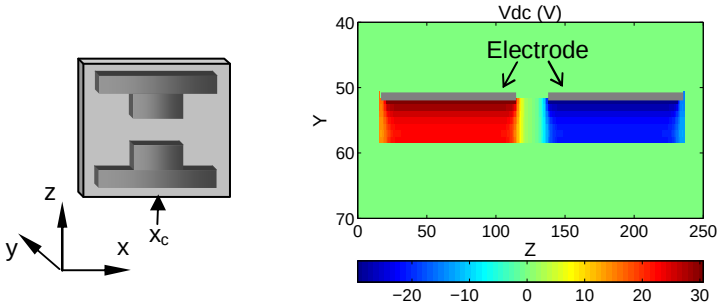

Figure 3: Distribution profiles of the steady-state internal potentials.

Once the steady-state electric field is obtained, the 3D discrete curl and carrier transport equations are applied to simulate the interaction between the antenna radiating structure and the device substrate. Immediately after fs-optical pulse excitation [see the inset in Fig. 4(a)], the temporal behavior can be observed by the current density. The instantaneous distributions of the electric field at 0.016 ps and 0.13 ps are shown in Fig. 4(b) for *yz*-plane and in Fig. 4(c) for *xz*-plane. The explanation to this transient field is that the carrier generated by the fs-optical pulse excitation induces the non-uniform photocurrent, which, in turn, will induce the field redistribution inside the gap area.

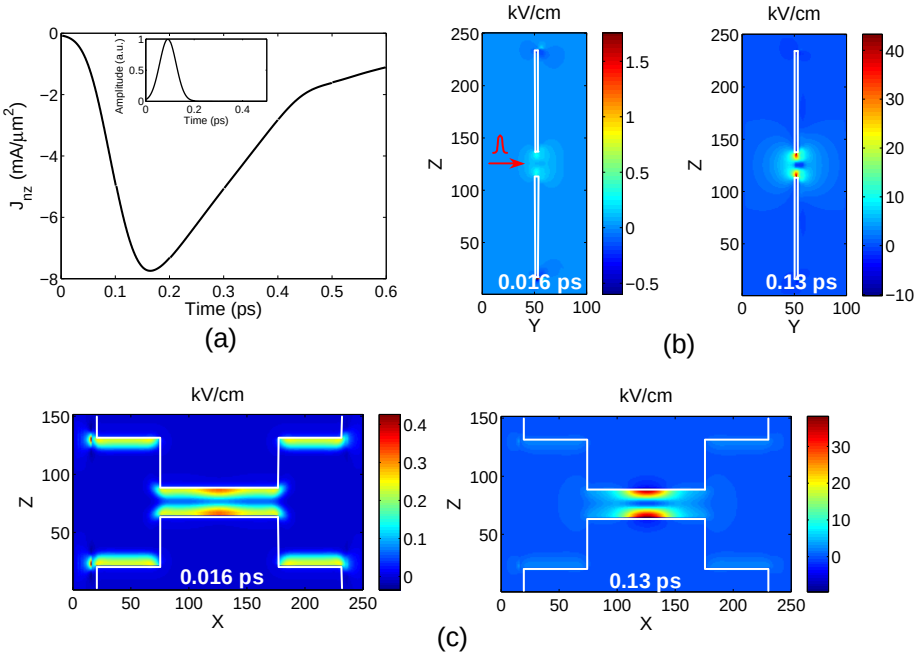

Figure 4: (a) Temporal behavior of the z-component current density and electric field distributions at 0.016 ps and 0.13 ps on (b) *yz*-plane and (c) *xz*-plane.

The next simulation performs the near field-to-far field transformation for the THz far-field radiation. Fig. 5 shows a reproduction of the waveforms from experimental data using our PC antenna model. The main positive peak of the temporal radiated field in Fig. 5(a) is attributed to the rises of the rising current by the photocarrier injection and the carrier acceleration under the bias

field in the PC antennas. The negative peak is attributed to the decay of the current governed by the carrier trapping times. Fig. 5(b) shows associated normalized frequency spectra of the radiated THz pulses in the frequency range of 0.1 to 3.5 THz. It is seen that the frequency spectral coverage is suitable for terahertz range applications. The frequency peak (~ 1.5 THz) is directly proportional to the effective length of the antenna electrode structure while the short carrier trapping time is responsible for the broad bandwidth.

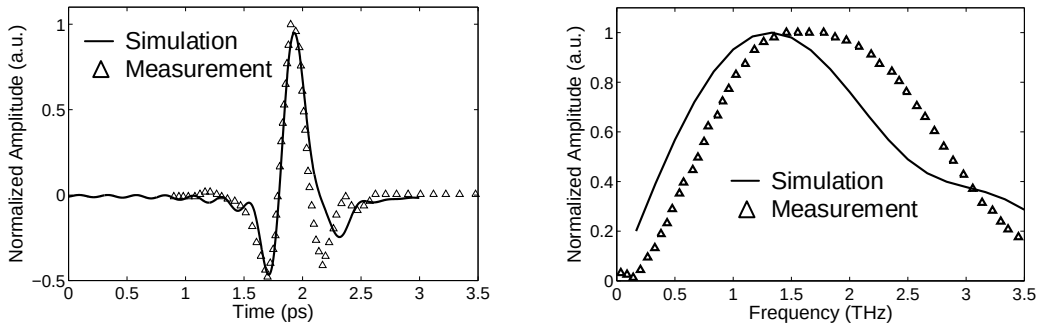

Figure 5: (a) Dynamics of THz emissions and (b) associated normalized frequency spectra.

4. Conclusion

A 3D full wave analysis with a consideration of field and device carrier interaction to improve PC antenna designs for generating THz pulses for broadband applications is described in this paper. The numerical models were implemented using Possion's equation for the steady-state device initialization, Maxwell's curl equations for the field-semiconductor device interaction, and near-field to far-field transformation for antenna emission. The numerical results and analysis show that the temporal and spatial behaviors of the field redistribution, carrier generation characteristics, and the photocurrent contribute to the nonlinear behavior of terahertz-pulse generation due to the laser induced bias voltage on the device. A proof of concept was verified by a reproduction of experimental data using the numerical model. The results using this scheme also show that the emitted terahertz frequency spectrum for broadband applications is proportional to the antenna electrode structure and the carrier trapping time of GaAs:As^+.

References

[1] P.R. Smith, D.H. Auston, M.C. Nuss, "Subpicosecond photoconducting dipole antennas," IEEE J. Quant. Elec., vol. 24, no. 2, pp. 255-260, 1988.

[2] Y. C. Shen, P. C. Upadhya, E. H. Linfield, H. E. Beere, and A. G. Davies, "Ultrabroadband terahertz radiation from low-temperature-grown GaAs photoconductive emitters," Appl. Phys. Lett., vol. 83, pp. 3117-3119, 2003.

[3] W.-C. Chen and C. S. Chang, "Structures and defects in arsenic-ion-implanted GaAs films annealed at high temperatures," J. Appl. Phys., vol. 81, pp. 7295-7300, 1997.

[4] J. Lloyd-Hughes, E. Castro-Camus, M. D. Fraser, C. Jagadish, and M. B. Johnston, "Carrier dynamics in ion-implanted GaAs studied by simulation and observation of terahertz emission," Phys. Rev. B, vol. 70, pp. 235330, 2004.

[5] D. Nolte, "Semi-insulating semiconductor heterostructures: Optoelectronic properties and applications," Appl. Phys. Rev., vol. 89, no. 9, pp. 6259-6289, May 1999.